Observation of Plasma Satellite Lines in Laser Produced Plasmas

D. Riley[1] and O. Willi[2]
[1]Department of Physics, The Queen's University of Belfast, Belfast BT7 1NN, Northern Ireland
[2]The Blackett Laboratory, Imperial College of Science Technology and Medicine, London SW7 2BZ, United Kingdom
(Received 31 July 1995)

The observation of satellite features to He-like emission lines from an aluminum plasma, generated with a short-pulse KrF laser system, is reported. There are interpreted as plasmon-induced satellites of the type described by Lee [J. Phys. B **12**, 1165 (1979)]. The plasma density inferred from line broadening is shown to be consistent with the electron density inferred from the frequency separation from line center.

PACS numbers: 52.50.Jm, 32.70.Jz, 52.70.La

Since their existence was first predicted by Mozer and Baranger [1], satellites to emission lines induced by collective plasma oscillations have been reported in low density plasmas and discussed by several authors [2–4]. In the original model, they are present when the plasma frequency (ω_p) is close to the separation between a dipole forbidden and an allowed transition and appear, spaced by ω_p, on either side of the forbidden line. Plasmon-induced satellites to hydrogenic lines (which cannot be modeled by the Mozer-Baranger theory) have also been reported [5]. The identification of similar spectral features in dense laser-produced plasmas is more problematic. Observations of short wavelength satellites to both H-like and He-like resonance lines of moderate Z elements have been reported [6,7], but the densities inferred from the position of these satellites were typically 10^{23} cm^{-3}, while density estimates from Stark broadening and dielectronic satellite ratios were around 2 orders of magnitude lower. Furthermore, Irons [8] has shown that these features can be interpreted as effects of the high opacity for resonance lines.

The purpose of this Letter is to report observations of satellite features to He-like Al lines in a short-pulse laser produced plasma. It will be seen that their appearance is consistent with modeling [9], in which the inclusion of nonthermal plasma oscillations in the impact approximation determination of Stark line profiles leads to a resonance at ω_p, on either side of the line center. The observations differ from previous ones in several ways. First, the satellites appear on either side of an optically thin line, thus precluding opacity effects. In addition, the spectra are temporally resolved and show that the satellites are present only during the laser pulse; this will be seen to be consistent with the modeling of their generation. It will also be shown that the electron density inferred from their spectral position is fairly consistent with simultaneous density estimates from Stark broadening of other lines in the same spectra. Finally, a possible explanation as to why these features appear in the present experiment and not in other data is considered.

The experimental conditions used in the generation and recording of the spectra were similar to those described in a previous publication [10], where good agreement between simulated and experimental emission characteristics was found. To summarize, 12 ps Raman amplified KrF laser pulses [11] at 268 nm were focused to a 50 μm spot onto solid targets, usually aluminum slabs, at irradiances of a few times 10^{15} W cm^{-2}. The H- and He-like K-shell emission was recorded with a crystal spectrometer coupled to an x-ray streak camera. The temporal and spectral ($\lambda/\delta\lambda$) resolutions were 10 ps and 350, respectively.

Figure 1 shows a digitized photograph of such a streaked spectrum, for average irradiance at pulse peak of 4×10^{15} W cm^{-2}. A satellite feature is clearly visible on the long wavelength side of the He-γ (Al XII $1s^2$-$1s4p$) line. On the short wavelength side, the satellite is less visible due to the broadened He-γ and He-δ (Al XII $1s^2$-$1s5p$) lines. Because of the instrument slit width, the entire duration of the feature appears to be around 30 ps. However, the measured temporal full width at half maximum (FWHM) is only 14 ps. Taking into account the instrument resolution, this implies a true FWHM duration of some 10 ps, which is similar to the laser pulse length. Figure 2 shows three density lineouts from the spectrum. Scan (i) is taken about 5 ps from

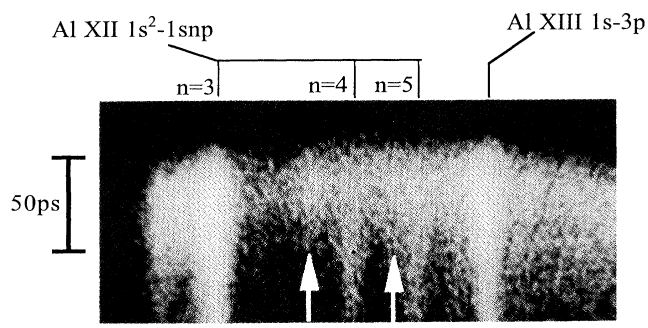

FIG. 1. Streaked spectrum for shot at irradiance $I = 4 \times 10^{15}$ W cm^{-2} on solid aluminum showing H-like and He-like K-shell emission. The arrows point to the observed satellite features.

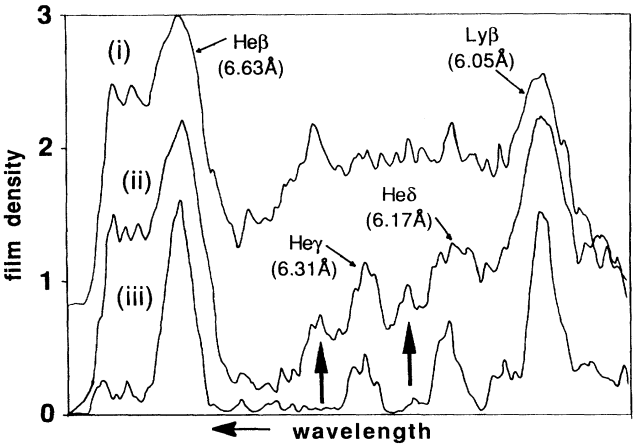

FIG. 2. Film density lineouts at (i) 5 ps, (ii) 15 ps, and (iii) 50 ps after the start of emission. Scan (i) has been shifted upwards by 0.8 in density for the sake of clarity in the diagram. The bold arrows indicate satellite features in scan (ii).

the start of emission, scan (ii) some 10 ps later, and scan (iii) some 50 ps after the first. Modeling of the x-ray emission suggests that, with the given instrument resolution, both scans (i) and (ii) should sample emission from around the pulse peak. In scan (ii), satellite features can be identified on either side of the He-γ line. A strong feature is also seen on the long wavelength side in scan (i), although, on the short wavelength side, merging with the He-δ line makes interpretation difficult. These features were consistently seen in other spectra taken under similar conditions. In scan (ii) the separation from the center of the He-γ line is symmetrical and is about 3×10^{16} s^{-1}, corresponding to an electron density of some 3×10^{23} cm^{-3}, if the usually small thermal correction term is neglected. It is important to establish that these features are not due either to a defect in the instrument or to dielectronic satellites. With regard to the former, by moving the crystal, a different dispersion is obtained with the spectral lines present in different parts of the cathode and satellite features evident in similar spectral positions. The short duration of the observed satellites seems to make dielectronic satellites unlikely as an explanation, although this in itself is not completely conclusive as these would be expected to have a short duration anyway. However, we note that the satellites to He-β can still be easily seen in scan (iii), some 50 ps after the start of emission. More importantly, for the He-γ line, the strongest dielectronic feature is expected to be some 9×10^{16} s^{-1} (60 eV) to the long wavelength side of the He-γ line. There is a feature at this position, which can be identified in all three scans, however, it is much weaker than the features of interest, thus indicating that dielectronic satellites do not explain the observed spectra. Furthermore, the feature on the short wavelength side of the He-γ line is at the wrong wavelength to be considered as a dielectronic satellite of the Ly-β line.

In Ref. [9], Lee describes how plasma satellites can be induced in the wings of hydrogenic emission lines when fast electrons, stopping in a plasma, give up energy to plasmons. In the strong microfields associated with the present plasma conditions, the He-like energy levels are effectively degenerate and linear Stark broadening occurs, so that they can be considered in the same way as hydrogenic lines. It is predicted that for a resonance in the far wings of the line, "bumps" in the profile will appear, while for the near wings "dips" in the profile are induced. This modeling shows that the effect is most evident on lines which have an unshifted central component, unaffected by the ion microfield, such as the H-like $1s$-$4p$ (Ly-γ) line. In particular, modeling of the Si XIII $1s^2$-$1s3p$ ^1P (He-β) line [9], at high density, shows very little modification to the profile. This is an important point as it means that we should only expect the satellites to be apparent on the He-γ line in our spectra, and also that the inference of electron density from the widths of the Al XII He-β and Ly-β (Al XIII $1s$-$3p$) lines made previously [10] and in the present work are not affected.

Turning to the possible source of fast electrons, we note that modeling of absorption data [12] for the same laser has highlighted the point that, even at normal incidence, there is a certain amount of resonance absorption resulting from the focusing geometry of the beam. For the present conditions the density scale length at the pulse peak is 1.8 μm, from hydrodynamic simulation. With an average angle of incidence of some 3.8°, it is estimated that approximately 8% of the incident laser light is absorbed by this mechanism. How much of this is channeled into fast electrons is harder to say, as this depends on the balance between collisional and nonlinear collisionless damping. At critical density the electron-ion collisional rate [13] is approximately $\nu_{ei} \sim 5 \times 10^{13}$ s^{-1} while simple modeling of the wave breaking rate gives $\nu_{\rm WB} \sim 2 \times 10^{14}$ s^{-1}, so that despite a large collisional damping we can estimate that a large fraction of resonantly absorbed energy goes into fast electrons, roughly 6% of incident energy. The hot electron temperature T_h can be estimated [14] to be about 4.9 keV, where $T_h = mv^2/2$ for fast electrons streaming into the plasma in planar geometry.

A time-dependent collisional radiative model [15] has been developed and used to postprocess the hydrodynamic data and account for line trapping on the strong resonance lines (Al XIII $1s$-$2p$ and Al XII $1s^2$-$1s2p$ ^1P) by use of both radiative transfer and Sobolev escape factors. The experimental line profile He-β and Ly-β transitions were compared to simulated profiles generated by convolving ionization data with a suite of line shape codes [16]. The inferred electron densities for K-shell emission agreed to better than 20% with the hydrodynamic simulation, confirming the conclusions about density and temperature found earlier [10]. Simulations with fast electrons included [15] indicated that they had little effect on ionization or excitation rates for the He- and H-like ions due to the relatively low value of T_h. Figure 3 shows the predicted emission profile at the peak of the pulse for the He-γ line. It can be seen that the He-γ emission also peaks at an electron density of about 1.7×10^{23} cm^{-3}, with 30% of the emission coming at higher density. The broken line represents the energy loss rate of fast electrons to the collective mode as they stream into the plasma. The stopping power equation used to calculate the electron energy for each cell and the contribution of collective effects is given by [17]

$$\frac{\partial E}{\partial x} = -\frac{2\pi e^4 N_e}{E} \ln\left(\frac{k_D v_0}{\omega_p}\right),$$

where E and v_0 are the electron energy and velocity, N_e is the electron density, ω_p is the plasma frequency, and k_D is the Debye wave number. This is a relatively simple model, and is strictly speaking only valid for the case when the velocity of the fast electrons greatly exceeds the thermal electron velocity. However, it is good enough to demonstrate that, for the laser-plasma conditions of our experiment, the fast electrons will lose a substantial part of their energy in the region of high emission for the He-like transitions, as can be seen in Fig. 3. We can estimate the energy density in the collective modes, W_{coll}, given the rate of fast electron generation and the stopping power. From Fig. 3, $W_{\mathrm{coll}} \sim 6 \times 10^{10}$ ergs cm^{-3}, which is about 3×10^{-4} times the thermal energy density in the region of maximum He-γ emission, the hot electron fraction at this point is of order 10^{-3}. The electric field associated with the fluctuations is estimated to be 4×10^8 V cm^{-1}, which is about one-tenth of the typical particle microfield.

The predicted density at which plasma turbulence is greatest agrees to within a factor of 2 with the experimentally inferred density from the satellite spacing. Including the thermal correction would bring slightly closer agreement.

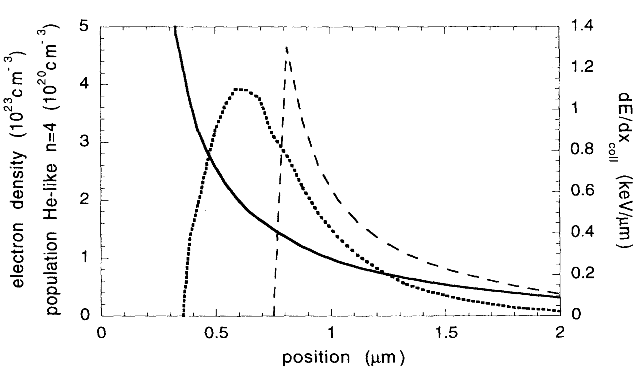

FIG. 3. The dotted line is the predicted population profile for the upper level of the He-γ transition at the peak of the laser pulse. The solid line denotes electron density, and the dashed line is the estimated loss rate to the collective mode for fast electrons with 4.9 keV initial energy.

We now turn to the question of why these features should be seen in the present data but not in other reported experiments. At longer wavelength, the hot electron temperature is higher than present and the emission density if not lower, is unlikely to be higher, and so coupling between plasma turbulence and x-ray emission is weaker. In the case of long pulses, the emission generally comes from much lower density than for short pulses, and fast electrons generated tend to lose energy in the higher density cold material, which does not strongly emit radiation. Also, if the spectra are time integrated, the relative intensity of a satellite feature will be much weaker than for time resolved data because of the longer emission times for resonance lines. A further criterion is that the spectral features are easy to interpret, such as the relatively simple He- and H-like line series. Thus we can conclude that the use of a short-pulse, short wavelength laser with time resolved spectra of K-shell emission enhances the change of observing these features.

A detailed modeling of the predicted plasma satellites would clearly be desirable. However, this is beyond the scope of this Letter. Dealing with the strong density and temperature gradients and a rigourous treatment of the fast electron propagation would make this a nontrivial task. The prediction of bumps or dips in the spectrum depends on the distance from line center and the enhancement of plasma modes. From experiment it is difficult to gauge the latter, since emission of the parent line comes from a range of plasma conditions, while the satellite emission will originate from some portion of this range.

Finally, we note that evidence for satellite features to the He-γ line was present in previously discussed spectra [10], although that publication did not address this issue. Examination of the spectrum displayed in Ref. [10] shows features, on the long wavelength side of the He-γ line, that could be identified as plasmon satellites with an inferred electron density of 1.7×10^{23} cm^{-3} and also features that could be identified as satellites at $2\omega_p$ with the same electron density. The latter are the more visible by virtue of being further from the broadened He-γ profile, but are weaker by a factor of about 3. Features on the short wavelength side could not be conclusively identified, due to emission from the higher He-like series members and the Ly-β line. The dipole selection rules would not preclude plasma satellites at $2\omega_p$, because the line is effectively hydrogenic. Since the modeling of the nonthermal contributions is to second order only in perturbation theory [9], it does not deal with this possibility, and so it is not possible to comment on the relative strength expected for satellites corresponding to higher harmonics of the plasma frequency, except to say that it is possible, given the estimate above, and the effect of continuum depression on energy levels, that the turbulent field could be a significant fraction of the net atomic binding field for the upper level of the transition in question.

In conclusion, we have observed satellite features to x-ray emission lines from a laser plasma that have the following properties. First, time resolution shows that they last only during the laser pulse. Second, the opacity of the parent line is low enough to prevent opacity effects being an issue. Third, the inferred electron density is consistent with that estimated from the widths of the He-β and Ly-β lines, which, consistent with theory, do not display obvious evidence for such satellites. Finally, consideration of the wavelength scaling for hot electron temperature and typical emission densities gives a plausible explanation for the appearance of these satellites in the present data when they are apparently absent from numerous previous experimental spectra.

Thanks are due to Dr. R. W. Lee and Professor D. D. Burgess for useful conversations and to L. A. Gizzi, S. M. Viana, F. Y. Khattak, and A. J. Mackinnon for their part in experiments. The authors also thank the staff of the Rutherford-Appleton Laboratory Laser division. This work was supported by a EPSRC/MoD grant.

[1] M. Baranger and B. Mozer, Phys. Rev. **123**, 25 (1961).
[2] H-J. Kunze and H. R. Griem, Phys. Rev. Lett. **21**, 1048 (1968).
[3] J. Hildebrandt and H-J. Kunze, Phys. Rev. Lett. **45**, 183 (1980).
[4] G. Bekefi, Comments Plasma Phys. Controlled Fusion **1**, 9 (1972); D. D. Burgess, J. Phys. B **4**, L7 (1971).
[5] T. A. Nee and H. R. Griem, Phys. Rev. A **14**, 1853 (1976).
[6] V. I. Bayanov, S. S. Gulidov, A. A. Mak, G. V. Peregudov, I. I. Sobel'man, A. D. Starikov, and V. A. Chirkov, Sov. J. Quantum Electron. **6**, 1226 (1976).
[7] V. A. Boiko, O. N. Krohkin, S. A. Pikuz, and A. Ya. Faenov, JETP Lett. **20**, 50 (1974).
[8] F. E. Irons, Aust. J. Phys. **33**, 25 (1980).
[9] R. W. Lee, J. Phys. B **12**, 1165 (1979).
[10] D. Riley, L. A. Gizzi, F. Y. Kahattak, A. J. Mackinnon, S. M. Viana, and O. Willi, Phys. Rev. Lett. **69**, 3739 (1992).
[11] M. J. Shaw, G. Bialolenker, G. J. Hirst, C. J. Hooker, M. H. Key, A. K. Kidd, J. M. D. Lister, and I. N. Ross, Opt. Lett. **18**, 1320 (1993).
[12] D. Riley, L. A. Gizzi, A. J. Mackinnon, S. M. Viana, and O. Willi, Phys. Rev. E **48**, 4855 (1993).
[13] W. L. Kruer, *Introduction to Laser Plasma Interactions* (Addison-Wesley, Reading, MA, 1988).
[14] D. W. Forslund, J. M. Kindel, and K. Lee, Phys. Rev. Lett. **39**, 284 (1977).
[15] D. Riley, Rutherford-Appleton Laboratory Report No. RAL-94-042, p. 77, 1994; A. Khan *et al.* Rutherford-Appleton Laboratory Report No. RAL-93-031, p. 79, 1993.
[16] R. W. Lee, J. Appl. Phys. **58**, 612 (1985).
[17] S. Ichimaru, *Basic Principles of Plasma Physics* (W. A. Benjamin, 1973), Chap. 4.

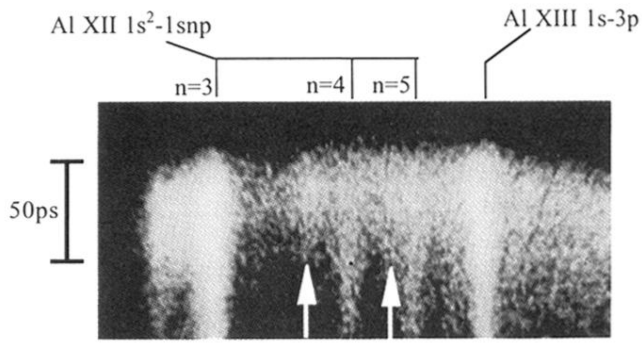

FIG. 1. Streaked spectrum for shot at irradiance $I = 4 \times 10^{15}$ W cm^{-2} on solid aluminum showing H-like and He-like K-shell emission. The arrows point to the observed satellite features.